DISCRETE AND CONTINUOUS
DYNAMICAL SYSTEMS SERIES B

doi:10.3934/dcdsb.2018064

# ION SIZE EFFECTS ON INDIVIDUAL FLUXES VIA POISSON-NERNST-PLANCK SYSTEMS WITH BIKERMAN'S LOCAL HARD-SPHERE POTENTIAL: ANALYSIS WITHOUT ELECTRONEUTRALITY BOUNDARY CONDITIONS

Hong Lu

School of Mathematics and Statistics
Shandong University, Weihai, Shandong 264209, China

Ji Li

School of Mathematics and Statistics
Huazhong University of Science and Technology, Wuhan, Hubei 430074, China

Joseph Shackelford, Jeremy Vorenberg and Mingji Zhang

Department of Mathematics
New Mexico Institute of Mining and Technology, Socorro, NM 87801, USA

(Communicated by Peter E. Kloeden)

Abstract. A quasi-one-dimensional steady-state Poisson-Nernst-Planck model with Bikerman's local hard-sphere potential for ionic flows of two oppositely charged ion species through a membrane channel is analyzed. Of particular interest is the qualitative properties of ionic flows in terms of individual fluxes *without the assumption of electroneutrality conditions*, which is more realistic to study ionic flow properties of interest. This is the novelty of this work. Our result shows that i) boundary concentrations and relative size of ion species play critical roles in characterizing ion size effects on individual fluxes; ii) the first order approximation $\mathcal{J}_{k1} = D_k J_{k1}$ in ion volume of individual fluxes $\mathcal{J}_k = D_k J_k$ is linear in boundary potential, furthermore, the signs of $\partial_V \mathcal{J}_{k1}$ and $\partial^2_{V\lambda} \mathcal{J}_{k1}$, which play key roles in characterizing ion size effects on ionic flows can be both negative depending further on boundary concentrations while they are always positive and independent of boundary concentrations under electroneutrality conditions (see Corollaries 3.2-3.3, Theorems 3.4-3.5 and Proposition 3.7). Numerical simulations are performed to identify some critical potentials defined in (2). We believe our results will provide useful insights for numerical and even experimental studies of ionic flows through membrane channels.

1. **Introduction.** One of the fundamental concerns of physiology is the function of ion channels. Ion channels are approximately cylindrical, hollow proteins with a hole down their middle that provides a controllable path for electro-diffusion of ions (mainly $Na^+$, $K^+$, $Ca^{++}$ and $Cl^-$) through biological membranes, establishing communications among cells and the external environment. In this way, ion channels

2010 *Mathematics Subject Classification.* Primary: 34A26, 34B16, 34D15; Secondary: 37D10, 92C35.

*Key words and phrases.* Ion channel, local hard-sphere potential, critical potentials, individual fluxes, electroneutrality conditions.

control a wide range of biological functions. Ionic flows are governed by fundamental physical laws of electrodiffusion which relate rates of quantities of interest. The macroscopic properties of ionic flows through ion channels rely further on external driving forces, namely, boundary potentials and concentrations of ion species involved; and specific structural characteristics, more precisely, the shape of its pore and the distribution of permanent charge along its interior wall. Two most relevant biological properties of a channel are permeation and selectivity, both of which are characterized by the current-voltage (I-V) relations measured experimentally under different ionic conditions.

Taking the structural characteristics into consideration, the basic continuum model for ionic flows is the Poisson-Nernst-Planck (PNP) system, which treats the aqueous medium (within which ions are migrating) as a dielectric continuum (see [3, 7, 12, 13, 15, 16, 17, 18, 19, 20, 25, 27, 28, 29, 37, 38, 42, 59], etc.). Under some reasonable conditions, the PNP system can be derived from more fundamental models such as the Langevin-Poisson system (see, for example, [14, 38, 55, 53, 59, 65]) or the Maxwell-Boltzmann equations (see, for example, [2, 37, 38, 59]), and from an energy variational analysis (see [34, 35, 36, 45, 67, 70]).

The simplest PNP model is the *classical* PNP (cPNP) system that contains only the *ideal* component of electrochemical potential. The cPNP system treats ions essentially as *point-charges*, and neglects ion size effects. It has been simulated (see, e.g., [6, 12, 13, 15, 25, 33]) and analyzed (see, e.g., [1, 4, 5, 9, 21, 22, 26, 40, 46, 47, 44, 51, 58, 63, 64, 66, 69]) to a great extent. However, a major weak point of the cPNP model is that ions are treated as point of charges, which is only reasonable in the extremely dilute setting. To study ion size effects on ionic flows, in particular, for ion species with the same valences but different ion sizes, for example, $Na^+$ (sodium) and $K^+$ (potassium), one has to consider excess (beyond the ideal) component in the electrochemical potential. One way is to include uncharged hard-sphere (HS) potentials to partially account for ion size effects. Physically, this means that each ion is approximated as a hard-sphere with its charges at the center of the sphere. Both local and nonlocal models for hard-sphere potentials were introduced for this purpose. Nonlocal models give the hard-sphere potentials as functionals of ion concentrations while local models depend pointwise on ion concentrations. An early local model for hard-sphere potentials was proposed by Bikerman ([8]), which is simple but unfortunately not ion specific (i.e., the hard-sphere potential is the same for different ion species). The Boublík-Mansoori-Carnahan-Starling-Leland local model is ion specific and has been shown to be accurate ([61, 62], etc.). Obviously, local models have the advantage of simplicity relative to nonlocal ones. The PNP models with ion sizes have been investigated computationally for ion channels and have shown great success (see [27, 28, 29, 31, 32, 34, 35, 36, 42, 54, 68, 70], etc.). Existence and uniqueness of minimizers and saddle points of the free-energy equilibrium formulation with ionic interaction have also been mathematically analyzed (see, for example, [23], [45]).

Recently, extending the approach in [21, 47], the authors of [41] studied a quasi-one-dimensional version of a steady-state PNP type system which involves two oppositely charged ions with zero permanent charge and a *local* model for the hard-sphere potential to account for finite ion size effects. In particular, an approximation of the I-V relation was derived by considering the ion sizes to be small parameters, more precisely, the authors treat $\varepsilon$ and $\nu = \nu_1$ as small parameters and derive approximations for the individual flux $\mathcal{J}_k$ and the current $\mathcal{I}$ expanded in $\nu$ with

$\lambda = \nu_2/\nu$ and fixed boundary concentrations $L_k$ and $R_k$ as follows (will be further discussed in Section 2):

$$\begin{aligned} \mathcal{J}_k =& D_k J_k = D_k J_{k0}(V;\varepsilon) + D_k J_{k1}(V;\lambda,\varepsilon)\nu + o(\nu), \\ \mathcal{I}(V;\varepsilon,d) =& z_1 D_1 \mathcal{J}_1 + z_2 D_2 \mathcal{J}_2 = I_0(V;\varepsilon) + I_1(V;\lambda,\varepsilon)\nu + o(\nu). \end{aligned} \tag{1}$$

This is crucial to further study the qualitative properties of ionic flows. It turns out that, for $k = 1, 2$, both $J_{k1}(V;\lambda,\varepsilon)$ and $I_1(V;\lambda,\varepsilon)$ are linear functions in $V$ (see (12) in Section 2.2). In particular, six critical potentials $V_{kc}$, $V_k^c$, $V_c$, $V^c$ are defined by

$$J_{k1}(V_{kc};\lambda,0) = 0, \quad I_1(V_c;\lambda,0) = 0, \quad \frac{d}{d\lambda} J_{k1}(V_k^c;\lambda,0) = 0, \quad \frac{d}{d\lambda} I_1(V^c;\lambda,0) = 0. \tag{2}$$

The significance of the six critical potentials is apparent from their definitions (See Theorems 4.8, 4.9, 4.18 and 4.19 in [41] for details), and from (1), *the sign of $\partial_V J_{k1}$ (resp. $\partial_{V\lambda} J_{k1}$, $\partial_V I_1$ and $\partial_{V\lambda} I$,) plays a key role in characterizing the effect from ion sizes.* Furthermore, the signs of those terms depend sensitively on multiple physical parameters, such as the boundary potentials and concentrations, ion valences, diffusion coefficients and ion sizes. The characterization of the distinct effects of the nonlinear interplay between these physical parameters will provide detailed information for one to better understand the flow property of interest.

With the assumption of *electroneutrality conditions* $z_1 L_1 = -z_2 L_2 = L$ and $z_1 R_1 = -z_2 R_2 = R$, and $L \neq R$, the authors in [41] established that

$$\partial_V I_1(V;\lambda,0) > 0 \ \text{ and } \ \partial^2_{V\lambda} I_1(V;\lambda,0) > 0.$$

Furthermore, the authors in [41] also provided a very special case showing that, for $z_1 = -z_2 = 1$ and fixed $L_2 > 0$, $\partial_V \mathcal{I}_1(V;\lambda,0) < 0$ if either $R_2 \geq R_1 \geq L_1 > 0$ and $\sqrt{L_1 L_2} > \sqrt{R_1 R_2}$, or $R_1 \geq L_1$, $R_2 < R_1$ and $\sqrt{L_1 L_2} > \mu^* \sqrt{R_1 R_2}$, where $\mu^* > 1$ is a constant.

Two interesting questions arising immediately are i) *in general, when $\partial_V I_1(V;\lambda,0)$ and $\partial_{V\lambda} I_1(V;\lambda,0)$ are negative?* ii) *Can the total flux be studied in terms of the individual fluxes $\mathcal{J}_k = D_k J_k$?*

To answer these questions, in this work, we study a quasi-one-dimensional PNP model with the same setting as that in [41] *except for the assumption of electroneutrality conditions.* Of particular interest is the sign study of $\partial_V J_{11}(V;\lambda,0)$ and $\partial_{V\lambda} J_{11}(V;\lambda,0)$ in terms of the individual flux. We take particular advantage of the work in [41] to provide a detailed explanation of how these physical parameters interact to produce a wide spectrum of behaviors for ionic flows. Our rigorous analysis (see Theorems 3.2-3.3, Corollaries 3.4-3.5 and Proposition 3.7) shows that

(i) boundary concentrations and relative size of ion species play critical roles in characterizing ion size effects on individual fluxes;

(ii) the first order approximation $\mathcal{J}_{k1} = D_k J_{k1}$ in ion volume of individual fluxes $\mathcal{J}_k = D_k J_k$ is linear in boundary potential, furthermore, the signs of $\partial_V \mathcal{J}_{k1}$ and $\partial^2_{V\lambda} \mathcal{J}_{k1}$ which play key roles in characterizing ion size effects on ionic flows can be both negative depending further on boundary concentrations while they are always positive and independent of boundary concentrations under electroneutrality conditions.

This is our main contribution in this work. To the best of the authors' knowledge, this work is the first analysis on roles that ion size plays in individual fluxes *without electroneutrality conditions.*

We emphasize that our results, for the relatively simple setting and assumptions of our model, are rigorous. *We believe these results will provide useful insights for numerical and even experimental studies of ionic flows through membrane channels.* It should be pointed out that the quasi-one-dimensional PNP model and the local hard-sphere model (see (7) below) adopted in [41] and in this paper are rather simple. Aside the trivial fact that they will miss the three-dimensional features of the problem, a major weakness is the missing of the excess electrostatic component in the excess potentials. Important phenomena such as charge inversion and layering may not be detected by this simple model.

The rest of the paper is organized as follows. In Section 2, we describe the quasi-one-dimensional PNP model of ion flows, a local model for hard-sphere (HS) potentials, the formulation of the boundary value problem of the singularly perturbed PNP-HS system, and the basic assumptions. Some results from [48] are recalled, and these will be the starting point of our study. In Section 3, *without the assumption of electroneutrality conditions*, we study the sign of $\partial_V J_{k1}$ (resp. $\partial_{V\lambda} J_{k1}$, $\partial_V I_1$ and $\partial_{V\lambda} I$), which plays a key role in characterizing the effect from ion sizes. It also turns out that the signs of those terms depend sensitively on multiple physical parameters such as boundary concentrations, ion valence and ion sizes. Partial orders of critical potentials identified in (2) are provided. Numerical simulations are performed to system (9)-(10) to identify some critical potentials defined in (2). The paper ends with a concluding remark provided in Section 4.

## 2. Models and some previous results.

In this section, we briefly recall the model of Poisson-Nernst-Planck (PNP) systems, and some main results obtained in [41] related to ion size effects on ionic flows.

### 2.1. A quasi-one-dimensional PNP system.

We assume the channel is narrow so that it can be effectively viewed as a one-dimensional channel that connects the interior and the exterior of the channel. A quasi-one-dimensional *steady-state* PNP model for ion flows of $n$ ion species though a single channel is (see [50, 52])

$$\begin{aligned} &\frac{1}{A(X)}\frac{d}{dX}\left(\varepsilon_r(X)\varepsilon_0 A(X)\frac{d\Phi}{dX}\right) = -e\left(\sum_{j=1}^{n} z_j C_j(X) + Q(X)\right), \\ &\frac{d\mathcal{J}_i}{dX} = 0, \quad -\mathcal{J}_i = \frac{1}{k_B T}\mathcal{D}_i(X)A(X)C_i(X)\frac{d\mu_i}{dX}, \quad i = 1, 2, \cdots, n, \end{aligned} \tag{3}$$

where $X \in [0, l]$, $e$ is the elementary charge, $k_B$ is the Boltzmann constant, $T$ is the absolute temperature; $\Phi$ is the electric potential, $Q(X)$ is the permanent charge of the channel, $\varepsilon_r(X)$ is the relative dielectric coefficient, $\varepsilon_0$ is the vacuum permittivity; $A(X)$ is the area of the cross-section of the channel over the point $X \in [0, l]$; for the $i$th ion species, $C_i$ is the concentration (number of $i$th ions per volume), $z_i$ is the valence (number of charges per particle) that is positive for cations and negative for anions, $\mu_i$ is the electrochemical potential, $\mathcal{J}_i$ is the flux density, and $\mathcal{D}_i(X)$ is the diffusion coefficient.

For system (3), we impose the following boundary conditions (see, [21] for justification), for $k = 1, 2, \cdots, n$,

$$\Phi(0) = \bar{V}, \quad C_i(0) = \mathcal{L}_i > 0; \quad \Phi(l) = 0, \quad C_i(l) = \mathcal{R}_i > 0. \tag{4}$$

For ion channels, an important characteristic is the so-called *I-V relations* (current-voltage relations). For a solution of the *steady-state* boundary value problem (3)-(4), the *rate of flow of charge through a cross-section* or *current* $\mathcal{I}$ is

$$\mathcal{I} = \sum_{j=1}^{n} z_j e \mathcal{J}_j. \tag{5}$$

For fixed boundary concentrations $\mathcal{L}_i$'s and $\mathcal{R}_i$'s, $\mathcal{J}_j$'s depend on $\bar{V}$ only and formula (5) provides a relation of the current $\mathcal{I}$ on the voltage $\bar{V}$. This relation is the I-V relation.

2.1.1. *Excess potential and a local hard sphere model.* The electrochemical potential $\mu_i(X)$ for the $i$th ion species consists of the ideal component $\mu_i^{id}(X)$ and the excess component $\mu_i^{ex}(X)$:

$$\mu_i(X) = \mu_i^{id}(X) + \mu_i^{ex}(X)$$

where

$$\mu_i^{id}(X) = z_i e \Phi(X) + k_B T \ln \frac{C_i(X)}{C_0} \tag{6}$$

with some characteristic number density $C_0$. The classical PNP system takes into consideration of the ideal component $\mu_i^{id}(X)$ only. This component reflects the collision between ion particles and the water molecules. It has been accepted that the classical PNP system is a reasonable model in, for example, the dilute case under which the ion particles can be treated as point particles and the ion-to-ion interaction can be more or less ignored. The excess chemical potential $\mu_i^{ex}(X)$ accounts for the finite size effect of charges (see, e.g., [60, 61]).

In this paper, we will take Bikerman's local hard-sphere model for $\mu_i^{ex}(X)$

$$\mu_i^{Bik}(X) = -k_B T \ln \left(1 - \sum_{j=1}^{n} \nu_j C_j(X)\right), \tag{7}$$

where $\nu_j$ is the volume of a *single* $j$th ion species. We would like to point out that since $C_j$ is the *number density* of $i$th ion species, it follows that $\sum_{j=1}^{n} \nu_j C_j < 1$. In this sense, Bikerman's LHS takes into consideration of nonzero ion sizes, however, it is not ion specific, more precisely, one has $\mu_1^{Bik}(X) = \mu_2^{Bik}(X) = \cdots = \mu_n^{Bik}(X)$ in our PNP model.

2.1.2. *The steady-state boundary value problem and assumptions.* The main goal of this paper is to examine the qualitative properties of the ion size effect on ionic flows via the steady-state PNP system (3)-(4). For definiteness, we will take essentially the same setting as that in [39], that is,

(A1). We consider two ion species ($n = 2$) with $z_1 > 0$ and $z_2 < 0$.
(A2). We assume the permanent charge $Q(X)$ to be zero.
(A3). For the electrochemical potential $\mu_i$, in addition to the ideal component $\mu_i^{id}(X)$ defined in (6), we also include a local hard-sphere potential (7) to approximate the excess component $\mu_i^{ex}(X)$.
(A4). The relative dielectric coefficient and the diffusion coefficient are constants, that is, $\varepsilon_r(X) = \varepsilon_r$ and $D_i(X) = D_i$.

In the sequel, we will assume (A1)–(A4). We first make a dimensionless rescaling following ([26]). Set $C_0 = \max\{\mathcal{L}_i, \mathcal{R}_i : i = 1, 2\}$ and let

$$\begin{aligned} \varepsilon^2 =& \frac{\varepsilon_r \varepsilon_0 k_B T}{e^2 l^2 C_0}, \quad x = \frac{X}{l}, \quad h(x) = \frac{A(X)}{l^2}, \quad D_i = l C_0 \mathcal{D}_i; \\ \phi(x) =& \frac{e}{k_B T} \Phi(X), \quad c_i(x) = \frac{C_i(X)}{C_0}, \quad J_i = \frac{\mathcal{J}_i}{D_i}; \end{aligned} \tag{8}$$

$$V = \frac{k_B T}{e}\bar{V}, \quad L_i = \frac{\mathcal{L}_i}{C_0}; \quad R_i = \frac{\mathcal{R}_i}{C_0}.$$

Using expressions (6) for the ideal component $\mu_i^{id}(X)$ and (7) for the excess chemical potential $\mu_i^{ex}(X)$, the boundary value problem (3)-(4) becomes

$$\begin{aligned}
&\varepsilon^2 \frac{d^2}{dx^2}\phi = -(z_1 c_1 + z_2 c_2), \quad \frac{dJ_i}{dx} = 0, \\
&\frac{dc_1}{dx} = -(z_1 - z_1\nu_1 c_1 - z_2\nu_2 c_2)c_1 \frac{d\phi}{dx} - \big(J_1 - (\nu_1 J_1 + \nu_2 J_2)c_1\big), \\
&\frac{dc_2}{dx} = -(z_2 - z_1\nu_1 c_1 - z_2\nu_2 c_2)c_2 \frac{d\phi}{dx} - \big(J_2 - (\nu_1 J_1 + \nu_2 J_2)c_2\big),
\end{aligned} \tag{9}$$

with boundary conditions, for $i = 1, 2$,

$$\phi(0) = V, \quad c_i(0) = L_i; \quad \phi(1) = 0, \quad c_i(1) = R_i. \tag{10}$$

To end this section, we would like to point out that

(i) for typical ion channel problems, physical range for the parameter $\varepsilon$ is $10^{-2} - 10^{-6}$, which is smaller for crowded ionic mixtures (large $C_0$) and larger for less crowded ionic mixtures. It is further assumed that the dimensionless parameters $\nu_i$'s are small; typical physical range for $\nu_i = v_i C_0$ is $10^{-2} - 10^{-4}$ with $10^{-2}$ corresponding to crowded ionic mixtures, say, $C_0 \sim 10$ M (molar) and with $10^{-4}$ to less crowded ionic mixtures, say, $C_0 \sim 100$ mM..

(ii) we take $h(x) = 1$ over the whole interval $[0, 1]$ in our analysis. This is because for ion channels with zero permanent charge, it turns out that the variable $h(x)$ contributes through an average, explicitly through the factor $\frac{1}{\int_0^1 h^{-1}(x)dx}$ (for example, the individual flux will be $\frac{D_k J_k}{\int_0^1 h^{-1}(x)dx}$, see [48]), which does not affect our analysis of the qualitative properties of the ionic flows.

2.2. **Some previous results.** We now recall some results obtained in [41], which are crucial for our study and which will be frequently used. In [41], the authors treat $\varepsilon$ and $\nu = \nu_1$ as small parameters and derive approximations for the current $\mathcal{I}$ and the individual flux $\mathcal{J}_k$ expanded in $\nu$ with $\lambda = \nu_2/\nu$ for $k = 1, 2$,

$$\begin{aligned}
\mathcal{I}(V;\varepsilon,\nu) =& z_1\mathcal{J}_1 + z_2\mathcal{J}_2 = I_0(V;\varepsilon) + I_1(V;\lambda,\varepsilon)\nu + o(\nu), \\
\mathcal{J}_k(V;\varepsilon,\nu) =& D_k J_{k0}(V;\varepsilon) + D_k J_{k1}(V;\lambda,\varepsilon)\nu + o(\nu),
\end{aligned} \tag{11}$$

where $\mathcal{J}_k = D_k J_k$, $J_{k0}$ is the zeroth order expansion in $\nu$, $J_{k1}$ is the first order expansion in $\nu$, and

$$\begin{aligned}
J_{10}(V;0) =& c_{10}^L - c_{10}^R + \frac{z_1(c_{10}^L - c_{10}^R)(\ln(L_1R_2) - \ln(L_2R_1))}{(z_1 - z_2)(\ln c_{10}^L - \ln c_{10}^R)} \\
&+ \frac{z_1(c_{10}^L - c_{10}^R)}{(\ln c_{10}^L - \ln c_{10}^R)} \frac{e}{k_B T} V,
\end{aligned}$$

$$\begin{aligned}
J_{20}(V;0) =& -\frac{z_1(c_{10}^L - c_{10}^R)}{z_2} - \frac{z_1(c_{10}^L - c_{10}^R)(\ln(L_1R_2) - \ln(L_2R_1))}{(z_1 - z_2)(\ln c_{10}^L - \ln c_{10}^R)} \\
&- \frac{z_1(c_{10}^L - c_{10}^R)}{(\ln c_{10}^L - \ln c_{10}^R)} \frac{e}{k_B T} V,
\end{aligned}$$

$$\begin{aligned} J_{11}(V;\lambda,0) =&\alpha_{10}(L_1,L_2,R_1,R_2,\lambda)+\alpha_{11}(L_1,L_2,R_1,R_2,\lambda)\frac{e}{k_BT}V,\\ J_{21}(V;\lambda,0) =&\beta_{10}(L_1,L_2,R_1,R_2,\lambda)+\beta_{11}(L_1,L_2,R_1,R_2,\lambda)\frac{e}{k_BT}V. \end{aligned} \tag{12}$$

In particular,

$$I_1(V;\lambda,0) =z_1D_1\alpha_{10}+z_2D_2\beta_{10}+(z_1D_1\alpha_{11}+z_2D_2\beta_{11})\frac{e}{k_BT}V. \tag{13}$$

Here,

$$\begin{aligned} \alpha_{10} =&\frac{\ln\frac{L_1R_2}{L_2R_1}+(z_1-z_2)(\ln c_{10}^L-\ln c_{10}^R)}{(z_1-z_2)(\ln c_{10}^L-\ln c_{10}^R)}\left[\frac{(z_1\lambda-z_2)\left((c_{10}^L)^2-(c_{10}^R)^2\right)}{2z_2}\right.\\ &\left.+c_{10}^L(L_1+\lambda L_2)-c_{10}^R(R_1+\lambda R_2)\right]\\ &+\frac{z_1(c_{10}^L-c_{10}^R)(R_1-L_1+\lambda(R_2-L_2))\ln\frac{L_1R_2}{L_2R_1}}{(z_1-z_2)\left(\ln c_{10}^L-\ln c_{10}^R\right)^2},\\ \alpha_{11} =&\frac{z_1c_{10}^L(L_1+\lambda L_2)-z_1c_{10}^R(R_1+\lambda R_2)}{\ln c_{10}^L-\ln c_{10}^R}+\frac{z_1(z_1\lambda-z_2)\left((c_{10}^L)^2-(c_{10}^R)^2\right)}{2z_2\left(\ln c_{10}^L-\ln c_{10}^R\right)}\\ &+\frac{z_1(c_{10}^L-c_{10}^R)(R_1-L_1+\lambda(R_2-L_2))}{\left(\ln c_{10}^L-\ln c_{10}^R\right)^2},\\ \beta_{10} =&-\frac{z_2\ln\frac{L_1R_2}{L_2R_1}+z_1(z_1-z_2)(\ln c_{10}^L-\ln c_{10}^R)}{z_2(z_1-z_2)(\ln c_{10}^L-\ln c_{10}^R)}\left[\frac{(z_1\lambda-z_2)\left((c_{10}^L)^2-(c_{10}^R)^2\right)}{2z_2}\right.\\ &\left.+c_{10}^L(L_1+\lambda L_2)-c_{10}^R(R_1+\lambda R_2)\right]\\ &-\frac{z_1(c_{10}^L-c_{10}^R)(R_1-L_1+\lambda(R_2-L_2))\ln\frac{L_1R_2}{L_2R_1}}{(z_1-z_2)\left(\ln c_{10}^L-\ln c_{10}^R\right)^2},\\ \beta_{11} =&-\alpha_{11}, \end{aligned} \tag{14}$$

where $c_{10}^L$ and $c_{20}^L$ are landing points given by

$$\begin{aligned} z_1c_{10}^L =&-z_2c_{20}^L=(z_1L_1)^{\frac{-z_2}{z_1-z_2}}(-z_2L_2)^{\frac{z_1}{z_1-z_2}},\\ z_1c_{10}^R =&-z_2c_{20}^R=(z_1R_1)^{\frac{-z_2}{z_1-z_2}}(-z_2R_2)^{\frac{z_1}{z_1-z_2}}. \end{aligned}$$

Under our setups, the critical potentials $V_{kc}$, $V_k^c$, $V_c$, and $V^c$ identified in (2) are given explicitly by

$$\begin{aligned} V_{1c} =&-\frac{k_BT}{e}\frac{\alpha_{10}}{\alpha_{11}},\quad V_1^c=-\frac{k_BT}{e}\frac{\alpha_{10,\lambda}}{\alpha_{11,\lambda}},\quad V_{2c}=\frac{k_BT}{e}\frac{\beta_{10}}{\alpha_{11}},\quad V_2^c=\frac{k_BT}{e}\frac{\beta_{10,\lambda}}{\alpha_{11,\lambda}},\\ V_c =&-\frac{k_BT}{e}\frac{z_1D_1\alpha_{10}+z_2D_2\beta_{10}}{z_1D_1\alpha_{11}+z_2D_2\beta_{11}},\quad V^c=-\frac{k_BT}{e}\frac{z_1D_1\alpha_{10,\lambda}+z_2D_2\beta_{10,\lambda}}{z_1D_1\alpha_{11,\lambda}+z_2D_2\beta_{11,\lambda}}. \end{aligned} \tag{15}$$

From (14) and (15), we observed that

**Lemma 2.1.** *Viewing $V_{kc}$, $V_k^c$, $V_c$ and $V^c$ as functions of $L_1, R_1$ with $-z_2L_2=\sigma(z_1L_1)$ and $-z_2R_2=\sigma(z_1R_1)$ for $k=1,2$, one has $V_{kc}$, $V_k^c$, $V_c$ and $V^c$ are homogeneous of degree zero in $(L_1,R_1)$, that is, for any $s>0$,*

$$V_{kc}(sL_1,sR_1)=V_{kc}(L_1,R_1),\quad V_k^c(sL_1,sR_1)=V_k^c(L_1,R_1),$$

$$V_c(sL_1, sR_1) = V_c(L_1, R_1), \quad \textit{and} \quad V^c(sL_1, sR_1) = V^c(L_1, R_1).$$

Note that, from (13) and (14), one has

$$\begin{aligned}
\partial_V I_1(V;\lambda,0) =& \frac{e}{k_BT}(z_1D_1 - z_2D_2)\partial_V J_{11}(V;\lambda,0)\\
=& \frac{e}{k_BT}(z_1D_1 - z_2D_2)\alpha_{11}(V;\lambda,0),\\
\partial^2_{V\lambda} I_1(V;\lambda,0) =& \frac{e}{k_BT}(z_1D_1 - z_2D_2)\partial^2_{V\lambda} J_{11}(V;\lambda,0)\\
=& \frac{e}{k_BT}(z_1D_1 - z_2D_2)\frac{\partial \alpha_{11}}{\partial \lambda}(V;\lambda,0).
\end{aligned} \tag{16}$$

To better answer the question imposed in the introduction, the first step is to study the the signs of $\partial_V J_{11}(V;\lambda,0) = \frac{e}{k_BT}\alpha_{11}(V;\lambda,0)$ and $\partial^2_{V\lambda} J_{11}(V;\lambda,0) = \frac{e}{k_BT}\frac{\partial \alpha_{11}}{\partial \lambda}(V;\lambda,0)$ in terms of the individual flux *without assuming the electroneutrality conditions.*

3. **Qualitative properties of ionic flows without electroneutrality conditions.** In this section, we would like to study the ion size effects on ionic flows without electroneutrality conditions. More precisely, we would like to study the sign of $\partial_V J_{k1}$ (resp. $\partial^2_{V\lambda} J_{k1}$, $\partial_V I_1$ and $\partial_{V\lambda} I_1$), which plays a key role in characterizing the effects on ionic flows from ion sizes.

Due to the difficulty in analysis, we will consider a relatively simple but more general (compared to the study in [41]) case with

$$-z_2L_2 = \sigma(z_1L_1) \quad \text{and} \quad -z_2R_2 = \sigma(z_1R_1) \tag{17}$$

for some positive constants $\sigma$, which is not equal to 1 ($\sigma = 1$ implies electroneutrality conditions on boundary concentrations). Under this assumption, one has $c^L_{10} = \sigma^{\frac{z_1}{z_1-z_2}}L_1$ and $c^R_{10} = \sigma^{\frac{z_1}{z_1-z_2}}R_1$. It follows form (12) and (14) that

$$\begin{aligned}
\partial_V J_{11}(V;\sigma;\lambda,0) =& \frac{e}{k_BT}\alpha_{11} = \frac{e}{k_BT}\frac{z_1\sigma^{\frac{z_1}{z_1-z_2}}(L_1^2 - R_1^2)}{\ln L_1 - \ln R_1}f(\sigma),\\
\partial_{V\lambda} J_{11}(V;\sigma;\lambda,0) =& \frac{e}{k_BT}\alpha_{11,\lambda} = -\frac{e}{k_BT}\frac{z_1^2}{z_2}\frac{\sigma^{\frac{2z_1}{z_1-z_2}}(L_1^2 - R_1^2)}{\ln L_1 - \ln R_1}\tilde{f}(\sigma),
\end{aligned} \tag{18}$$

where

$$\begin{aligned}
f(\sigma) =& \lambda\frac{z_1}{-z_2}(1-m)\sigma + \frac{z_1\lambda - z_2}{2z_2}\sigma^{\frac{z_1}{z_1-z_2}} + 1 - m,\\
\tilde{f}(\sigma) =& (1-m)\sigma^{\frac{-z_2}{z_1-z_2}} - \frac{1}{2},
\end{aligned} \tag{19}$$

where

$$m = \frac{1}{L_1 + R_1}\frac{L_1 - R_1}{\ln L_1 - \ln R_1} \tag{20}$$

To get started, we establish the following result, which will be used frequently in our analysis.

**Lemma 3.1.** *For $L_1 \neq R_1$, one has $m = \frac{1}{L_1+R_1}\frac{L_1-R_1}{\ln L_1 - \ln R_1} \in (0, \frac{1}{2})$. As $L_1 \to R_1$, $m \to \frac{1}{2}$.*

*Proof.* For convenience, for $L_1 \neq R_1$, we define $m = m(L_1, R_1) = \frac{1}{L_1+R_1}\frac{L_1-R_1}{\ln L_1 - \ln R_1}$ Let $x = \frac{L_1}{R_1}$, we have $m(x) = \frac{x-1}{(x+1)\ln x}$, $x > 0$. Direct calculations give

$$m'(x) = \frac{n(x)}{[(x+1)\ln x]^2}, \quad \text{where} \quad n(x) = 2\ln x - x + \frac{1}{x}.$$

For $n(x)$, one has $n'(x) = -\frac{(x-1)^2}{x^2} \leq 0$; and $n''(x) = \frac{2(1-x)}{x^3}$. It follows that

$$n'(1) = 0,\ n''(1) = 0,\ n''(x) > 0 \Longleftrightarrow 0 < x < 1;\ \text{and}\ n''(x) < 0 \Longleftrightarrow x > 1.$$

Hence, $m'(x) > 0$ if $0 < x < 1$; and $m'(x) < 0$ if $x > 1$. Note that $m(x) \to 0$ as $x \to 0$; and $m(x) \to 0$ as $x \to \infty$. Therefore, $m(x)$ has its global maximum at $x = 1$ (that is, as $L_1 \to R_1$), which is $\frac{1}{2}$. This completes the proof. □

3.1. **Signs of $\partial_V J_{k1}$ and $\partial^2_{V\lambda} J_{k1}$.** It is clear from (12) that the sign of $\partial_V J_{k1}$ (resp. $\partial^2_{V\lambda} J_{k1}$, $k = 1, 2$ plays an important role in characterizing the size effects on ionic flows. It is worth analyzing it in details. Note that, from (12) and (14), one has

$$\partial_V J_{11} = -\partial_V J_{21} \quad \text{and} \quad \partial^2_{V\lambda} J_{11} = -\partial^2_{V\lambda} J_{21}.$$

Therefore, we will mainly focus on the study of the individual flux $J_{11}$. We first consider the sign of $\partial_V J_{11}$.

**Corollary 3.2.** *Assume $L_1 \neq R_1$. Then, there exist $\lambda_1^*$ and $\lambda_2^*$, two distinct real roots of $h(\lambda) = \frac{z_1}{z_2}\ln\lambda + \left(1 - \frac{z_1}{z_2}\right)\ln(z_1\lambda - z_2) - \left(1 - \frac{z_1}{z_2}\right)\ln 2(z_1 - z_2)$ with $\lambda_1^* < \lambda_2^*$ such that*

*(I) for either $0 < \lambda < \lambda_1^*$ or $\lambda > \lambda_2^*$, there exist two distinct real roots of $f(\sigma) = 0$, denoted by $\sigma_{1*}$ and $\sigma_{2*}$ with $\sigma_{1*} < \sigma_c < \sigma_{2*}$ such that $\partial_V J_{11}(V;\sigma;\lambda,0) > 0$ if either $0 < \sigma < \sigma_{1*}$ or $\sigma > \sigma_{2*}$; and $\partial_V J_{11}(V;\sigma;\lambda,0) < 0$ if $\sigma_{1*} < \sigma < \sigma_{2*}$, where $\sigma_c = \left(\frac{2(z_1-z_2)\lambda(1-m)}{z_1\lambda - z_2}\right)^{\frac{z_1-z_2}{z_2}}$ is the unique critical point of $f(\sigma)$.*

*(II) for $\lambda_1^* < \lambda < \lambda_2^*$, there exists $m^* \in (0, \frac{1}{2})$ such that*
*(II-1) with $0 < m < m^*$, $\partial_V J_{11}(V;\sigma;\lambda,0) > 0$ for $\sigma > 0$;*
*(II-2) with $m^* < m < \frac{1}{2}$, $\partial_V J_{11}(V;\sigma;\lambda,0) > 0$ if either $0 < \sigma < \sigma_1^*$ or $\sigma > \sigma_2^*$ and $\partial_V J_{11}(V;\sigma;\lambda,0) < 0$ if $\sigma_1^* < \sigma < \sigma_2^*$, where $\sigma_1^*$ and $\sigma_2^*$ are two distinct real roots of $f(\sigma) = 0$.*

*Proof.* Note that the sign of $\partial_V J_{11}(V;\sigma;\lambda,0)$ is determined by the sign of $f(\sigma)$ since

$$\frac{e}{k_B T} > 0 \text{ and } \sigma^{\frac{z_1}{z_1-z_2}}\frac{L_1^2 - R_1^2}{\ln L_1 - \ln R_1} > 0 \text{ for } \sigma > 0 \text{ and } L_1 \neq R_1 \text{ (even as } L_1 \to R_1).$$

From equation (19), direct calculations give

$$f'(\sigma) = \frac{z_1\lambda}{-z_2}(1 - z_1 m) + \frac{z_1^2\lambda}{2z_2(z_1 - z_2)}\sigma^{\frac{z_2}{z_1-z_2}} \quad \text{and} \quad f''(\sigma) = \frac{z_1(z_1\lambda - z_2)}{2(z_1 - z_2)^2}\sigma^{\frac{2z_2-z_1}{z_1-z_2}}.$$

It is easy to see that $f''(\sigma) > 0$ for $\sigma > 0$, which implies that $f(\sigma)$ is concave up for $\sigma > 0$. It follows that $f(\sigma)$ has a global minimum at some point $\sigma_c$, which is the unique solution of $f'(\sigma) = 0$. It is given by $\sigma_c = \left(\frac{2(z_1-z_2)\lambda(1-z_1 m)}{z_1\lambda - z_2}\right)^{\frac{z_1-z_2}{z_2}}$.

Note that $f(0+) = 1 - m > 0$ since from Lemma 3.1, $0 < m < \frac{1}{2}$ for $L_1 \neq R_1$. It is clear that $f(\sigma)$ obtains its global minimum at $\sigma = \sigma_c$, which is given by

$$f(\sigma_c) = -\frac{z_1\lambda - z_2}{2(z_1 - z_2)} \left( \frac{2(z_1 - z_2)\lambda(1-m)}{z_1\lambda - z_2} \right)^{\frac{z_1}{z_2}} + 1 - m.$$

We now consider the sign of $f(\sigma_c)$. For convenience, we redefine the quantity $f(\sigma_c)$ as a function of $m$, denoted by $g(m)$. Note that $z_1 \geq 1$ and $z_2 \leq -1$. Careful calculations give

$$g'(m) = -1 + \frac{z_1}{z_2} \left( \frac{z_1\lambda - z_2}{2(z_1 - z_2)} \right)^{1 - \frac{z_1}{z_2}} \lambda^{\frac{z_1}{z_2}} (1-m)^{\frac{z_1}{z_2} - 1} < 0, \ 0 < m < \frac{1}{2}.$$

Note also that

$$g(0+) = 1 - \left( \frac{z_1\lambda - z_2}{2(z_1 - z_2)} \right)^{1 - \frac{z_1}{z_2}} \lambda^{\frac{z_1}{z_2}}. \tag{21}$$

One can easily check that $g(0+) > 0$ if $\lambda_1^* < \lambda < \lambda_2^*$, and $g(0+) < 0$ if either $0 < \lambda < \lambda_1^*$ or $\lambda > \lambda_2^*$ where $\lambda_1^*$ and $\lambda_2^*$ are two distinct real roots of

$$h(\lambda) = \frac{z_1}{z_2} \ln \lambda + \left(1 - \frac{z_1}{z_2}\right) \ln(z_1\lambda - z_2) - \left(1 - \frac{z_1}{z_2}\right) \ln 2(z_1 - z_2). \tag{22}$$

We next study the sign of $g(m)$ for two cases.

**Case I.** $g(0+) < 0$. It is easy to check that $g(m) < 0$ for $0 < m < \frac{1}{2}$ since $g(m)$ is decreasing for $0 < m < \frac{1}{2}$. This implies $f(\sigma_c) < 0$. Therefore, there exist two distinct real roots of $f(\sigma) = 0$, denoted by $\sigma_{1*}$ and $\sigma_{2*}$ with $\sigma_{1*} < \sigma_{2*}$ such that $f(\sigma) > 0$ if $0 < \sigma < \sigma_{1*}$ or $\sigma > \sigma_{2*}$, and $f(\sigma) < 0$ if $\sigma_{1*} < \sigma < \sigma_{2*}$. It follows that, with $0 < \lambda < \lambda^*$, $\partial_V J_{11}(V; \sigma; \lambda, 0) < 0$ for $\sigma_{1*} < \sigma < \sigma_{2*}$, and $\partial_V J_{11}(V; \sigma; \lambda, 0) > 0$ for $0 < \sigma < \sigma_{1*}$ or $\sigma > \sigma_{2*}$.

**Case II.** $g(0+) > 0$**.** Note that

$$g(\frac{1}{2}-) = \frac{1}{2} \left( 1 - \left( \frac{z_1\lambda - z_2}{z_1 - z_2} \right)^{1 - \frac{z_1}{z_2}} \lambda^{\frac{z_1}{z_2}} \right).$$

One has $g(\frac{1}{2}-) < 0$ if and only if $k(\lambda) > 0$, where

$$k(\lambda) = \frac{z_1}{z_2} \ln \lambda + \left(1 - \frac{z_1}{z_2}\right) \ln(z_1\lambda - z_2) - \left(1 - \frac{z_1}{z_2}\right) \ln(z_1 - z_2).$$

Direct calculations give

$$k'(\lambda) = \frac{z_1(\lambda - 1)}{\lambda(z_1\lambda - z_2)}, \text{ for } \lambda > 0.$$

Hence, $k'(\lambda) > 0$ if $\lambda > 1$, $k'(\lambda) < 0$ if $0 < \lambda < 1$. Furthermore, $\lambda = 1$ is the unique critical point of $k(\lambda)$, where $k(\lambda)$ has its global minimum. It is given by $k(1) = 0$. This implies $k(\lambda) \geq 0$ for $\lambda > 0$. It follows that $g(\frac{1}{2}-) < 0$. Therefore, we have $g(0+) > 0$ and $g(\frac{1}{2}-) < 0$ for $\lambda_1^* < \lambda < \lambda_2^*$, and there exists $m^* \in (0, \frac{1}{2})$ such that $g(m) > 0$ if $0 < m < m^*$, and $g(m) < 0$ if $m^* < m < \frac{1}{2}$. That is,

$$f(\sigma_c) > 0 \text{ if } 0 < m < m^*, \text{ and } f(\sigma_c) < 0 \text{ if } m^* < m < \frac{1}{2}.$$

Hence, $f(\sigma) > 0$ if $0 < m < m^*$ for $\sigma > 0$; and if $m^* < m < \frac{1}{2}$, there exist two distinct real roots of $f(\sigma) = 0$ denoted by $\sigma_1^*$ and $\sigma_2^*$ with $\sigma_1^* < \sigma_2^*$ such that $f(\sigma) < 0$ if $\sigma_1^* < \sigma < \sigma_2^*$, and $f(\sigma) > 0$ if $0 < \sigma < \sigma_1^*$ or $\sigma > \sigma_2^*$. Therefore,

(i) $\partial_V J_{11}(V;\sigma;\lambda,0) > 0$ either for $\sigma > 0$ with $0 < m < m^*$, or for $0 < \sigma < \sigma_1^*$ or $\sigma > \sigma_2^*$ with $m^* < m < \frac{1}{2}$;

(ii) $\partial_V J_{11}(V;\sigma;\lambda,0) < 0$ for $\sigma_1^* < \sigma < \sigma_2^*$ with $m^* < m < \frac{1}{2}$. This completes the proof. □

A similar argument leads to the result related to the sign of $\partial_{V\lambda} J_{11}$.

**Corollary 3.3.** *Assume $L_1 \neq R_1$. Then, $\partial^2_{V\lambda} J_{11}(V;\lambda,0) > 0$, if $\sigma > \bar{\sigma}$, and $\partial^2_{V\lambda} J_{11}(V;\lambda,0) < 0$, if $0 < \sigma < \bar{\sigma}$, where $\bar{\sigma} = \big(2(1-m)\big)^{\frac{z_1 - z_2}{-z_2}}$ is the unique real root of $\tilde{f}(\sigma) = 0$.*

Together with (2), the following results can be established.

**Theorem 3.4.** *Assume $L_1 \neq R_1$. For small $\epsilon > 0$ and $\nu > 0$, one has*

- *(i) for either $0 < \lambda < \lambda_1^*$ or $\lambda > \lambda_2^*$,*
  - *(i-1) for either $0 < \sigma < \sigma_{1*}$ or $\sigma > \sigma_{2*}$, $J_{11}(V;\sigma;\lambda,\nu) > J_{11}(V;\sigma;\lambda,0)$ (resp. $J_{11}(V;\sigma;\lambda,\nu) < J_{11}(V;\sigma;\lambda,0)$) if $V > V_{1c}$ (resp. $V < V_{1c}$), that is, the ion size enhances (resp. reduces) the individual flux;*
  - *(i-2) for $\sigma_{1*} < \sigma < \sigma_{2*}$, $J_{11}(V;\sigma;\lambda,\nu) > J_{11}(V;\sigma;\lambda,0)$ (resp. $J_{11}(V;\sigma;\lambda,\nu) < J_{11}(V;\sigma;\lambda,0)$) if $V < V_{1c}$ (resp. $V > V_{1c}$), that is, the ion size enhances (resp. reduces) the individual flux.*
- *(ii) for $\lambda_1^* < \lambda < \lambda_2^*$,*
  - *(ii-1) with $0 < m < m^*$, for $\sigma > 0$, $J_{11}(V;\sigma;\lambda,\nu) > J_{11}(V;\sigma;\lambda,0)$ ($J_{11}(V;\sigma;\lambda,\nu) < J_{11}(V;\sigma;\lambda,0)$), that is, the ion size enhances (resp. reduces) the individual flux, if $V > V_{1c}$ (resp. $V < V_{1c}$);*
  - *(ii-2) with $m^* < m < \frac{1}{2}$,*
    - *(ii-2-a) for either $0 < \sigma < \sigma_1^*$ or $\sigma > \sigma_2^*$, $J_{11}(V;\sigma;\lambda,\nu) > J_{11}(V;\sigma;\lambda,0)$ (resp. $J_{11}(V;\sigma;\lambda,\nu) < J_{11}(V;\sigma;\lambda,0)$), that is, the ion size enhances (resp. reduces) the individual flux if $V > V_{1c}$ (resp. $V < V_{1c}$);*
    - *(ii-2-b) for $\sigma_1^* < \sigma < \sigma_2^*$, $J_{11}(V;\sigma;\lambda,\nu) > J_{11}(V;\sigma;\lambda,0)$ (resp. $J_{11}(V;\sigma;\lambda,\nu) < J_{11}(V;\sigma;\lambda,0)$), that is, the ion size enhances (resp. reduces) the individual flux if $V < V_{1c}$ (resp. $V > V_{1c}$).*

**Theorem 3.5.** *Assume $L_1 \neq R_1$. For small $\epsilon > 0$ and $\nu > 0$, one has*

- *(i) for $\sigma > \bar{\sigma}$, $J_{11}(V;\sigma;\lambda,\nu)$ is increasing (resp. decreasing) in $\lambda$ if $V > V_1^c$ (resp. $V < V_1^c$) ;*
- *(ii) for $0 < \sigma < \bar{\sigma}$, $J_{11}(V;\sigma;\lambda,\nu)$ is increasing (resp. decreasing) in $\lambda$ if $V < V_1^c$ (resp. $V > V_1^c$).*

In particular,

**Proposition 3.6.** *As $L_1 \to R_1$, one has*

- *(i) For $\lambda \neq 1$, there exist two distinct real roots of $f(\sigma) = 0$, denoted by $\sigma^{(1)}$ and $\sigma^{(2)}$ with $\sigma^{(1)} < \sigma^{(2)}$ such that $\partial_V J_{11}(V;\sigma;\lambda,0) > 0$ if either $0 < \sigma < \sigma^{(1)}$ or $\sigma > \sigma^{(2)}$; and $\partial_V J_{11}(V;\sigma;\lambda,0) < 0$ if $\sigma^{(1)} < \sigma < \sigma^{(2)}$. Furthermore, for $\lambda = 1$, $\partial_V J_{11}(V;\sigma;\lambda,0) \geq 0$ for all $\sigma > 0$.*
- *(ii) $\partial^2_{V\lambda} J_{11}(V;\lambda,0) > 0$, if $\sigma > 1$, and $\partial^2_{V\lambda} J_{11}(V;\lambda,0) < 0$, if $0 < \sigma < 1$.*

To show the existence of those particular values of $\sigma$, $\lambda$ and $m$ in Theorem 3.2, we provide the following example. **Example.** We take $z_1 = -z_2 = 1$. Numerically, we obtain Figures 1, 2 and 3, respectively.

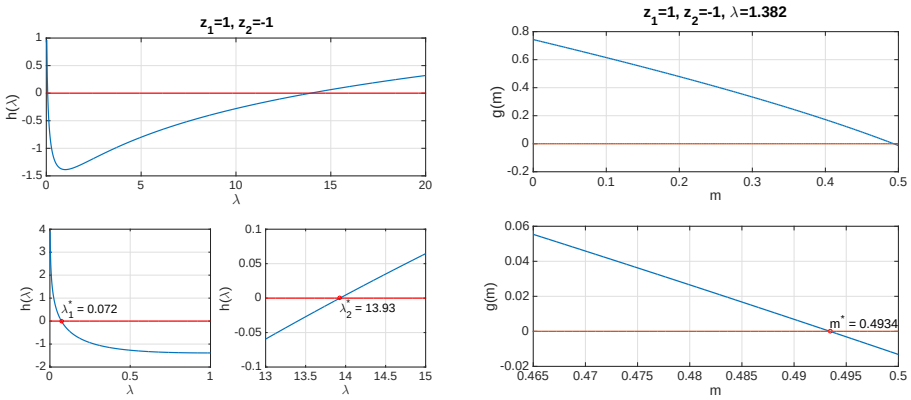


FIGURE 1. Numerical detection of critical values for $\lambda$ (left graph) and $m$ (right one) in Theorem 3.2.

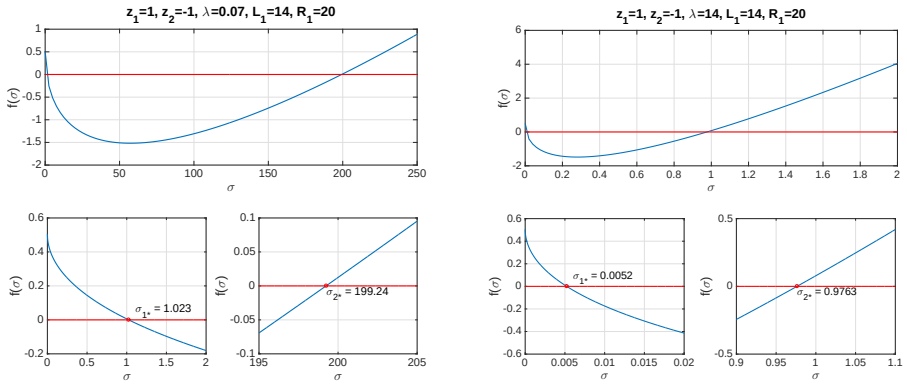


FIGURE 2. Numerical detection of critical values for $\sigma$, which corresponds to statement (I) in Theorem 3.2. The left graph is for $\lambda < \lambda_1^* = 0.072$, and the right one is for $\lambda > \lambda_2^* = 13.93$.

We next would like to point out that

**Proposition 3.7.** *Under electroneutrality conditions* $z_1L_1 + z_2L_2 = 0$ *and* $z_1R_1 + z_2R_2 = 0$, *for* $L_1 \neq R_1$, *one has* $\partial_V J_{11}(V;\lambda,0) > 0$ *and* $\partial^2_{V\lambda} J_{11}(V;\lambda,0) > 0$.

*Proof.* Upon introducing $z_1L_1 = -z_2L_2 = L$ and $z_1R_1 = -z_2R_2 = R$, one has

$$c_{10}^L = L_1 = \frac{1}{z_1}L,\ c_{20}^L = L_2 = \frac{1}{-z_2}L,\ c_{10}^R = R_1 = \frac{1}{z_1}R \text{ and } c_{20}^R = R_2 = \frac{1}{-z_2}R.$$

By careful calculations, we obtain

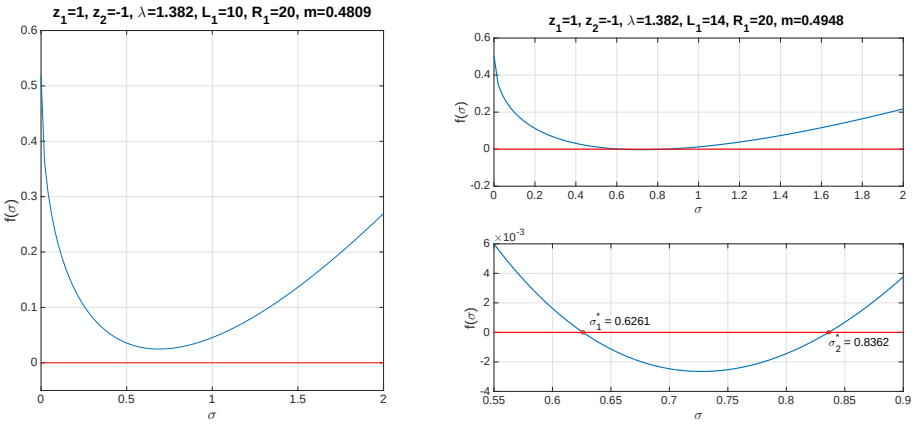


FIGURE 3. Numerical detection of critical values $\sigma$ corresponding to statement (II) in Theorem 3.2 with $\lambda_1^* < \lambda < \lambda_2^*$. The left graph is for $0 < m < m^* = 0.4934$, and the right one is for $m^* < m < \frac{1}{2}$.

$$\partial_V J_{11}(V;\lambda,0) = \frac{e}{k_B T}\frac{(\lambda z_1 - z_2)(L+R)}{z_1 z_2}\frac{L-R}{\ln L - \ln R}\left(m - \frac{1}{2}\right),$$
$$\partial^2_{V\lambda} J_{11}(V;\lambda,0) = \frac{e}{k_B T}\frac{L+R}{z_2}\frac{L-R}{\ln L - \ln R}\left(m - \frac{1}{2}\right).$$

Notice that $\frac{e}{k_B T} > 0$, $z_2 < 0$ and $\frac{L-R}{\ln L - \ln R} > 0$. Together with $m < \frac{1}{2}$ from Lemma 3.1, one has $\partial_V J_{11}(V;\lambda,0) > 0$ and $\partial^2_{V\lambda} J_{11}(V;\lambda,0) > 0$. This completes the proof. □

**Remark 3.8.** Proposition 3.7 is a special case of Theorems 3.2-3.3 with $\sigma = 1$.

To end this section, we would like to comment that since $\alpha_{11} = -\beta_{11}$ in (14), one has $\partial_V J_{11} = -\partial_V J_{21}$ and $\partial^2_{V\lambda} J_{11} = -\partial^2_{V\lambda} J_{21}$. Corresponding results related to $J_{21}$ can be easily obtained, and we leave them to the readers.

3.2. **Sign studies related to the total flux.** Some qualitative properties of the total flux (the total flow rate of charge) in terms of $I_1 = z_1 D_1 J_{11} + z_2 D_2 J_{21}$ have been studied in [41]. In particular, under the assumption of electroneutrality conditions, the author established that $\partial_V I_1(V;\lambda,0) > 0$ (resp. $\partial^2_{V\lambda} I_1(V;\lambda,0) > 0$ ), which implies that, for small $\varepsilon > 0$ and

However, there are not too much discussion about the negativeness of these terms except a very special case stated in our introduction.

From (16), the study of the signs of $\partial^2_{V\lambda} I_1(V;\lambda,0)$ and $\partial_V I_1(V;\lambda,0)$ follows directly from our analysis of the individual fluxes (Theorem 3.8 and Theorem 3.14). More precisely,

**Proposition 3.9.** *Under assumption* (17)*, one has*

$$\partial^2_{V\lambda} I_1(V;\lambda,0)\partial^2_{V\lambda} J_{11}(V;\lambda,0) > 0; \text{ and } \partial_V I_1(V;\lambda,0)\partial_V J_{11}(V;\lambda,0) > 0.$$

3.3. **Partial orders of critical potentials.** Our main interest in this section is to provide a partial order for the critical potentials identified in (2) (see [41] for more details). We first consider the critical potentials $V_{1c}$, $V_{2c}$ and $V_c$ that balance the ion size effects on both the individual flux and the total flux.

For the six critical potentials, $V_{kc}$, $V_k^c$ related to the individual fluxes, and $V_c$, $V^c$ related to the total flux, given by (15) (see also [41]), it is expected that $V_c$ and $\hat{V}_c$ depend on $V_{1c}$ and $V_{2c}$, and $V^c$ and $\hat{V}^c$ depend on $V_1^c$ and $V_2^c$. More precisely,

**Corollary 3.10.** *We have*

$$V_c = \frac{z_1 D_1 V_{1c} - z_2 D_2 V_{2c}}{z_1 D_1 - z_2 D_2}, \quad V^c = \frac{z_1 D_1 V_1^c - z_2 D_2 V_2^c}{z_1 D_1 - z_2 D_2}.$$

*Proof.* It follows from the relation (14) and the expressions of the six critical potentials in (15) directly. We omit it here. □

The following result can be established.

**Proposition 3.11.** *Assume (17) and $L_1 < R_1$. Assume further that $\alpha_{11} > 0$. With $\lambda_1^*$ and $\lambda_2^*$ as given in Theorem 3.2,*

*(i) for $\lambda_1^* < \lambda < \lambda_2^*$, one has $V_{2c} < V_c < V_{1c}$;*

*(ii) for either $0 < \lambda < \lambda_1^*$ or $\lambda > \lambda_2^*$, there exist two distinct real roots $\bar{\sigma}_1$ and $\bar{\sigma}_2$ with $\bar{\sigma}_1 < \bar{\sigma}_2$ of $p(\sigma) = \frac{z_1\lambda}{-z_2}\sigma + \frac{z_1\lambda - z_2}{2z_2}\sigma^{\frac{z_1}{z_2}} + 1 = 0$ such that $V_{2c} < V_c < V_{1c}$ if either $0 < \sigma < \bar{\sigma}_1$ or $\sigma > \bar{\sigma}_2$; and $V_{1c} < V_c < V_{2c}$ if $\bar{\sigma}_1 < \sigma < \bar{\sigma}_2$.*

*Proof.* We only provide the proof for the case with $\alpha_{11} > 0$. Similar argument can be easily applied to the case with $\alpha_{11} < 0$.

From (15) and Corollary 3.10, one has

$$V_{2c} - V_{1c} = \frac{k_B T}{e}\frac{1}{\alpha_{11}}\left(1 - \frac{z_1}{z_2}\right)(L_1^2 - R_1^2)p(\sigma),$$
$$\text{where } p(\sigma) = \frac{z_1\lambda}{-z_2}\sigma + \frac{z_1\lambda - z_2}{2z_2}\sigma^{\frac{z_1}{z_2}} + 1.$$

Direct calculations give

$$p'(\sigma) = \frac{z_1\lambda}{-z_2} + \frac{z_1(z_1\lambda - z_2)}{2z_2(z_1 - z_2)}\sigma^{\frac{z_2}{z_1 - z_2}} \text{ and } p''(\sigma) = \frac{z_1(z_1\lambda - z_2)}{2(z_1 - z_2)^2}\sigma^{\frac{2z_2 - z_1}{z_1 - z_2}} > 0 \text{ for } \sigma > 0.$$

In particular, $\tilde{\sigma} = \left(\frac{2(z_1 - z_2)\lambda}{z_1\lambda - z_2}\right)^{\frac{z_1 - z_2}{z_2}}$ is the unique critical point of $p(\sigma)$ for $\sigma > 0$. $p(\sigma)$ has its absolute minimum at $\sigma = \tilde{\sigma}$, which is given by

$$p(\tilde{\sigma}) = 1 - \left(\frac{z_1\lambda - z_2}{2(z_1 - z_2)}\right)^{1 - \frac{z_1}{z_2}} \lambda^{\frac{z_1}{z_2}}.$$

Notice that $p(\tilde{\sigma}) = g(0+)$, where $g(0+)$ is given in (21). It follows that $p(\tilde{\sigma}) > 0$ if $\lambda_1^* < \lambda < \lambda_2^*$; and $p(\tilde{\sigma}) < 0$ if either $0 < \lambda < \lambda_1^*$ or $\lambda > \lambda_2^*$, where $\lambda_1^*$ and $\lambda_2^*$ are two distinct real roots of (22).

Together with $p(0+) = 1 > 0$ , one has

(i) with $\lambda_1^* < \lambda < \lambda_2^*$, $V_{2c} - V_{1c} < 0$ since $p(\sigma) > 0$ for all $\sigma > 0$.

(ii) with either $0 < \lambda < \lambda_1^*$ or $\lambda > \lambda_2^*$, there exist two distinct real roots $\bar{\sigma}_1$ and $\bar{\sigma}_2$, say $\bar{\sigma}_1 < \bar{\sigma}_2$, of $p(\sigma) = 0$ such that $p(\sigma) > 0$ if either $0 < \sigma < \bar{\sigma}_1$ or $\sigma > \bar{\sigma}_2$; and $p(\sigma) < 0$ if $\bar{\sigma}_1 < \sigma < \bar{\sigma}_2$. Thus, $V_{2c} - V_{1c} < 0$ if either $0 < \sigma < \bar{\sigma}_1$ or $\sigma > \bar{\sigma}_2$; and $V_{2c} - V_{1c} > 0$ if $\bar{\sigma}_1 < \sigma < \bar{\sigma}_2$.

Note also that

$$V_c - V_{1c} = \frac{z_2 D_2 (V_{1c} - V_{2c})}{z_1 D_1 - z_2 D_2} \quad \text{and} \quad V_c - V_{2c} = \frac{z_1 D_1 (V_{1c} - V_{2c})}{z_1 D_1 - z_2 D_2}.$$

One has $V_{1c} < V_c < V_{2c}$ if $V_{2c} - V_{1c} > 0$; and $V_{2c} < V_c < V_{1c}$ if $V_{2c} - V_{1c} < 0$.

This completes the proof. □

Similarly, for the critical potentials $V_1^c$, $V_2^c$ and $V^c$ that separate the relative size effects on both the individual flux and the total flux, we have

**Proposition 3.12.** *Assume (17) and $L_1 < R_1$. Assume further that $\alpha_{11,\lambda} > 0$. Then, for $\sigma > 2^{\frac{z_1 - z_2}{z_2}}$, one has $V_2^c < V^c < V_1^c$, and for $\sigma < 2^{\frac{z_1 - z_2}{z_2}}$, one has $V_1^c < V^c < V_2^c$.*

*Proof.* The proof is straightforward, and we omit it here. □

**Remark 3.13.** Similar results can be obtained for the case with $\alpha_{11} < 0$ and $\alpha_{11,\lambda} < 0$, respectively. We leave it to readers.

To end this section, we perform numerical simulations to system (9)-(10) directly to numerically identify the six critical potentials given in (15) and to further examine our analytical result established in Theorem 3.2 and Corollary 3.4 (see Figure 4).

In our numerical simulations, we take $14 = L_1 < R_1 = 20$ (implying $m(L_1, R_1) = 0.4948 > m^* = 0.4934$) and $0.072 = \lambda_1^* < \lambda = 1.38 < \lambda_2^* = 13.93$. For small $\epsilon = 0.001$, our numerical result shows that $V_{2c} < V_c < V_{1c}$, and $V_2^c < V^c < V_1^c$, which is consistent with our analytical ones stated in Proposition 3.11 and Proposition 3.12. We comment that those critical potentials split the potential region into several subregions, and over each subregion, the ion size effects on ionic flows will be different. This provides a possible way to control the boundary potential to produce desired properties of ionic flows while the boundary concentration and relative ion sizes satisfy certain conditions. Take $V_{2c} < V_c < V_{1c}$ (the critical potentials that balance ion size effects) for example, from Theorem 3.4 and Proposition 3.9, one has, for small $\epsilon > 0$ and small $\nu > 0$,

(S1) for $V < V_{2c}$, $\mathcal{J}_1(V;\nu) < \mathcal{J}_1(V;0)$, $\mathcal{J}_2(V;\nu) > \mathcal{J}_2(V;0)$, and $\mathcal{I}(V;\nu) < \mathcal{I}(V;0)$;

(S2) for $V_{2c} < V < V_c$, $\mathcal{J}_1(V;\nu) < \mathcal{J}_1(V;0)$, $\mathcal{J}_2(V;\nu) < \mathcal{J}_2(V;0)$, and $\mathcal{I}(V;\nu) < \mathcal{I}(V;0)$;

(S3) for $V_c < V < V_{1c}$, $\mathcal{J}_1(V;\nu) < \mathcal{J}_1(V;0)$, $\mathcal{J}_2(V;\nu) < \mathcal{J}_2(V;0)$, and $\mathcal{I}(V;\nu) > \mathcal{I}(V;0)$;

(S4) for $V > V_{1c}$, $\mathcal{J}_1(V;\nu) > \mathcal{J}_1(V;0)$, $\mathcal{J}_2(V;\nu) < \mathcal{J}_2(V;0)$, and $\mathcal{I}(V;\nu) > \mathcal{I}(V;0)$.

In particular, in (S3) and (S3), the ion size reduce both the individual fluxes $\mathcal{J}_1$ and $\mathcal{J}_2$, however, the effect on the total flow rate of charge $\mathcal{I}$ is opposite. Recall that $\mathcal{I}(V;\nu,\lambda) - \mathcal{I}_0(V)$, $\mathcal{J}_1(V;\nu,\lambda) - \mathcal{J}_{10}(V)$ and $\mathcal{J}_2(V;\nu,\lambda) - \mathcal{J}_{20}(V)$ are all linear functions in the potential $V$, (S1)-(S4) can be further verified by our numerical simulations in Figure 4 (left column).

To find the critical potentials $V_1^c$, $V_2^c$ and $V^c$, our numerical approach is a numerical interpretation of the following analytical result (taking the individual flux $J_1$ for example). For fixed $(\lambda^*, \nu^*)$, we define

$$H(V,\lambda) = J_1(V;\lambda,\nu^*) - J_1(V;\lambda^*,\nu^*).$$

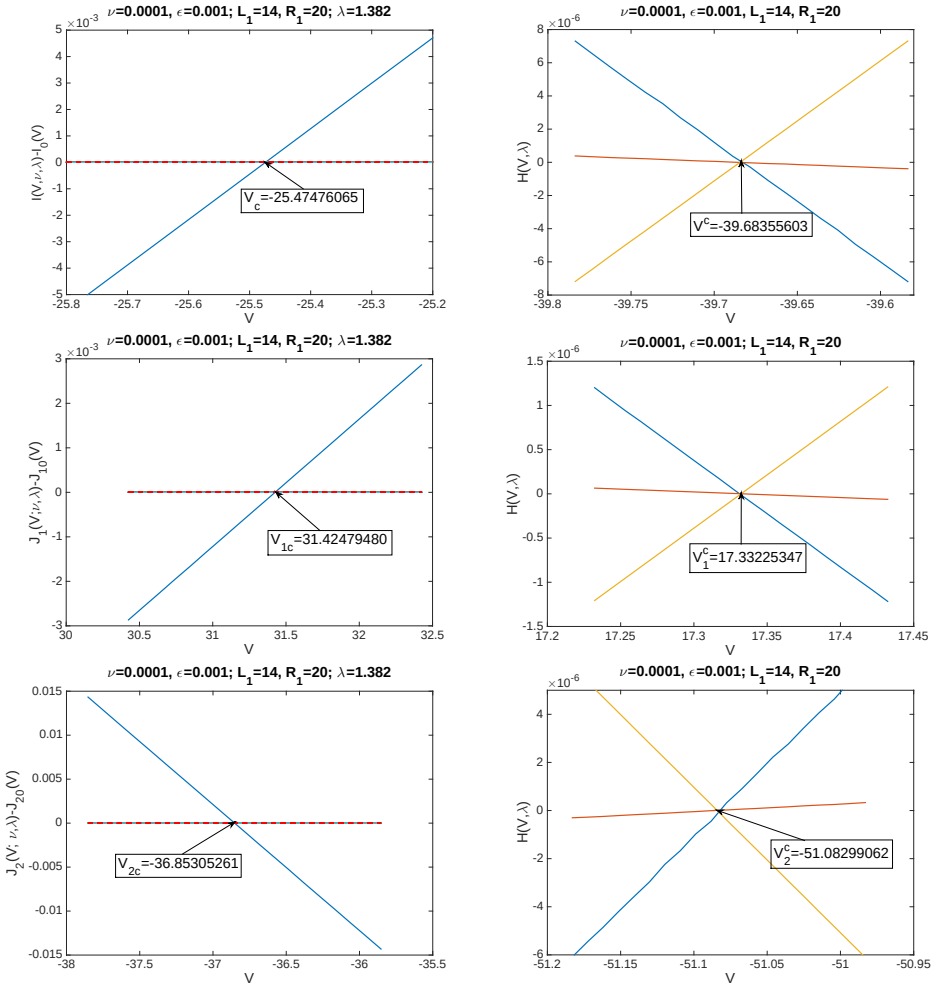


FIGURE 4. Numerical identification of six critical potentials in (15) with $z_1 = -z_2 = 1$. In the left column, the vertical axis actually represents, from top to bottom, $\mathcal{I}(V;\nu,\lambda) - \mathcal{I}_0(V)$, $\mathcal{J}_1(V;\nu,\lambda) - \mathcal{J}_{10}(V)$ and $\mathcal{J}_2(V;\nu,\lambda) - \mathcal{J}_{20}(V)$, respectively. In particular, the x-axis for all figures actually represents $\frac{e}{k_B T} V$.

**Proposition 3.14.** *For fixed $(\lambda,\nu) = (\lambda^*,\nu^*)$, $V_1^{c*}$ is the value defined in (2) if and only if the point $(V_1^{c*},\lambda^*)$ is a saddle point of $H(V,\lambda)$ under the condition that $\partial^2_{V\lambda} H(V_1^{c*},\lambda^*) = \partial^2_{V\lambda} J_1(V_1^{c}*,\lambda^*) \neq 0$.*

*Proof.* Notice that $H(V,\lambda^*) = 0$ for all $V$. Hence, $H_V(V,\lambda^*) = H_{VV}(V,\lambda^*) = 0$. From the definition of $V_1^{c*}$, one has $H_\lambda(V_1^{c*},\lambda^*) = J_{1,\lambda}(V_1^{c*};\lambda^*,\nu^*) = 0$, which implies that $(V_1^{c*},\lambda^*)$ is a critical point of $H(V,\lambda)$. Following from

$$\left(\frac{\partial^2 H}{\partial V^2}\frac{\partial^2 H}{\partial \lambda^2} - \left(\frac{\partial^2 H}{\partial V \partial \lambda}\right)^2\right)(V_1^{c*},\lambda^*) = -\left(\frac{\partial^2 H}{\partial V \partial \lambda}\right)^2 (V_1^{c*},\lambda*) < 0,$$

one concludes that $(V_1^{c*},\lambda^*)$ is a saddle point of $H(V,\lambda)$. □

It follows that, for fixed $(\lambda^*, \nu^*)$, one can numerically compute $J_1(V; \lambda, \nu^*)$, and hence $H(V, \lambda)$ for any $\lambda$ close to $\lambda^*$, then apply Proposition 3.14 to estimate $V_1^{c*}$ from the saddle point of $H(V, \lambda)$. In our numerical simulations, we fix $\lambda^* = \lambda/3$ and plot $H(V, \lambda)$ as a function of $V$ with three different $\lambda$ values (see the second column in Figure 4 for $J_1, J_2$ and $I$). Our analytical results for zeroth order in $\varepsilon$ and first order in $\nu$ tell us that the graphs for these three different $\lambda$ values should have a common intersection point with $V = V_1^c$.

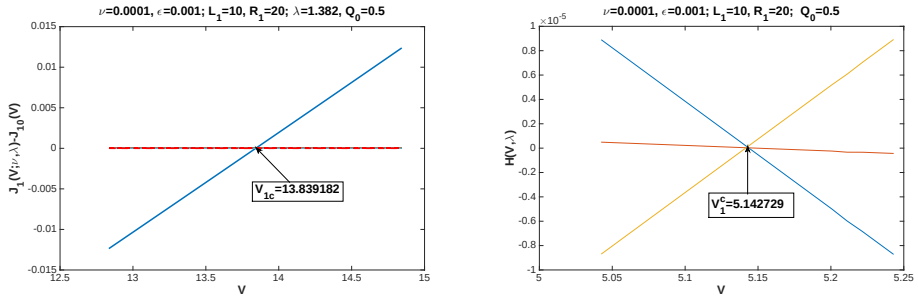


FIGURE 5. Numerical identification of critical potentials $V_{1c}$ and $V_1^c$ for individual flux $\mathcal{J}_1$ with $z_1 = -z_2 = 1$ and nonzero permanent charge. The x-axis for all figures actually represents $\frac{e}{k_B T} V$.

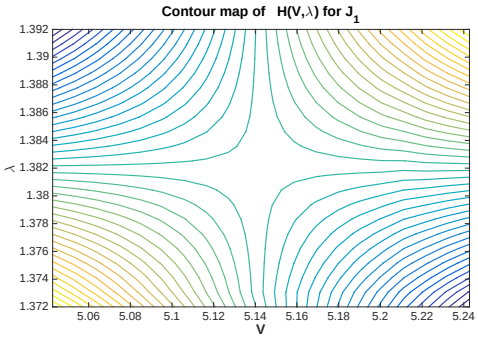


FIGURE 6. Numerical approximations of critical potentials $V_1^c$ for individual flux $\mathcal{J}_1$ with $z_1 = -z_2 = 1$ and nonzero permanent charge as illustrated in Proposition 3.14. The x-axis for all figures actually represents $\frac{e}{k_B T} V$.

4. **Concluding Remarks.** In this work, we consider the PNP model with local excess chemical potentials to account for finite size effects on ionic flows for two ion species, one positively charged and one negatively charged. The qualitative properties of ionic flows, in terms of *individual fluxes*, are studied *without the assumption of electroneutrality conditions*, which is more realistic, and it turns out that these properties depend very sensitively on boundary concentrations (in terms of $m(L_1, R_1)$) and relative ion sizes (in terms of $\lambda$) in addition to other physical parameters such as boundary potentials, ion valences and ion sizes. Our result shows

that the first order approximation $\mathcal{J}_{k1} = D_k J_{k1}$ in ion volume of individual fluxes $\mathcal{J}_k = D_k J_k$ is linear in boundary potential, and the signs of $\partial_V \mathcal{J}_{k1}$ and $\partial^2_{V\lambda} \mathcal{J}_{k1}$ which play key roles in characterizing ion size effects on ionic flows can be both negative depending further on boundary concentrations while they are always positive and independent of boundary concentrations under electroneutrality conditions. This is the novelty of our work. For the relatively simple setting and assumptions of the model studied in this paper, we are able to characterize the distinct effects of the nonlinear interplay between these physical parameters. The dynamical behaviors of ionic flows studied in this work are much more rich compared to those in [41] under electroneutrality conditions.

Finally, we comment that the model studied in this paper is oversimplified and the specific setting (such as zero permanent charge assumption) of our problem may not reflect precisely any realistic biological settings. However, we believe the existence of these critical potentials are generally in valid (even for PNP model with nonzero permanent charge, see Figures 5 and 6 for $V_{1c}$ and $V_1^c$ with nonzero permanent charge $Q(x)$ defined piecewise by $Q(x) = 0$ if $x \in [0, 1/3] \cup [2/3, 1]$ and $Q(x) = Q_0$ if $x \in [1/3, 2/3]$, where $Q_0 = 0.5$) and the awareness of the potential existence of these critical voltage itself would be useful for further numerical studies and stimulate further analytical studies of ionic flows through ion channels. We believe our results will provide useful insights for numerical and even experimental studies of ionic flows through membrane channels.

**Acknowledgments.** H. Lu was supported in part by the NSF of China (No.11601278 and No.11601274), the PSF of China (No. 2016M592172) and the NSF of Shandong Province (No. 2016ZRE27099). M. Zhang was supported by start-up funds for new faculties at New Mexico Institute of Mining and Technology.

## REFERENCES

[1] N. Abaid, R. S. Eisenberg and W. Liu, Asymptotic expansions of I-V relations via a Poisson-Nernst-Planck system, *SIAM J. Appl. Dyn. Syst.,* **7** (2008), 1507–1526.

[2] V. Barcilon, Ion flow through narrow membrane channels: Part I, *SIAM J. Appl. Math.,* **52** (1992), 1391–1404.

[3] D. Boda, D. Busath, B. Eisenberg, D. Henderson and W. Nonner, Monte Carlo simulations of ion selectivity in a biological Na+ channel: Charge-space competition, *Phys. Chem. Chem. Phys.,* **4** (2002), 5154–5160.

[4] V. Barcilon, D.-P. Chen and R. S. Eisenberg, Ion flow through narrow membrane channels: Part II, *SIAM J. Appl. Math.,* **52** (1992), 1405–1425.

[5] V. Barcilon, D.-P. Chen, R. S. Eisenberg and J. W. Jerome, Qualitative properties of steady-state Poisson-Nernst-Planck systems: Perturbation and simulation study, *SIAM J. Appl. Math.,* **57** (1997), 631–648.

[6] M. Burger, R. S. Eisenberg and H. W. Engl, Inverse problems related to ion channel selectivity, *SIAM J. Appl. Math.,* **67** (2007), 960–989.

[7] D. Boda, D. Gillespie, W. Nonner, D. Henderson and B. Eisenberg, Computing induced charges in inhomogeneous dielectric media: application in a Monte Carlo simulation of complex ionic systems, *Phys. Rev. E,* **69** (2004), 046702 (1–10).

[8] J. J. Bikerman, Structure and capacity of the electrical double layer, *Philos. Mag.,* **33** (1942), 384–397.

[9] P. W. Bates, Y. Jia, G. Lin, H. Lu and M. Zhang, Individual flux study via steady-state Poisson-Nernst-Planck systems: Effects from boundary conditions, *SIAM J. Appl. Dyn. Syst.,* **16** (2017), 410–430.

[10] P. W. Bates, W. Liu, H. Lu and M. Zhang, Ion size and valence effects on ionic flows via Poisson-Nernst-Planck models, *Commu. Math. Sci.,* **15** (2017), 881–901.

[11] J. H. Chaudhry, S. D. Bond and L. N. Olson, Finite Element Approximation to a Finite-Size Modified Poisson-Boltzmann Equation, *J. Sci. Comput*, **47** (2011), 347–364.

[12] A. E. Cardenas, R. D. Coalson and M. G. Kurnikova, Three-dimensional poisson-nernst-planck theory studies: Influence of membrane electrostatics on gramicidin a channel conductance, *Biophys. J.*, **79** (2000), 80–93.
[13] D. P. Chen and R. S. Eisenberg, Charges, currents and potentials in ionic channels of one conformation, *Biophys. J.*, **64** (1993), 1405–1421.
[14] S. Chung and S. Kuyucak, Predicting channel function from channel structure using Brownian dynamics simulations, *Clin. Exp. Pharmacol Physiol.*, **28** (2001), 89–94.
[15] R. Coalson and M. Kurnikova, Poisson-Nernst-Planck theory approach to the calculation of current through biological ion channels, *IEEE Transaction on NanoBioscience,* **4** (2005), 81–93.
[16] B. Eisenberg, Ion channels as devices, *J. Comp. Electro.*, **2** (2003), 245–249.
[17] B. Eisenberg, Proteins, channels, and crowded ions, *Biophys. Chem.*, **100** (2003), 507–517.
[18] R. S. Eisenberg, Channels as enzymes, *J. Memb. Biol.*, **115** (1990), 1–12.
[19] R. S. Eisenberg and A. Biology, Electrostatics and Ionic Channels, *In New Developments and Theoretical Studies of Proteins, R. Elber, Editor,* 269–357, World Scientific, Philadelphia, 1996.
[20] R. S. Eisenberg, From structure to function in open ionic channels, *J. Memb. Biol.,* **171** (1999), 1–24.
[21] B. Eisenberg and W. Liu, Poisson-Nernst-Planck systems for ion channels with permanent charges, *SIAM J. Math. Anal.,* **38** (2007), 1932–1966.
[22] B. Eisenberg, W. Liu and H. Xu, Reversal permanent charge and reversal potential: Case studies via classical Poisson-Nernst-Planck models, *Nonlinearity,* **28** (2015), 103–127.
[23] A. Ern, R. Joubaud and T. Leliévre, Mathematical study of non-ideal electrostatic correlations in equilibrium electrolytes, *Nonlinearity*, **25** (2012), 1635–1652.
[24] J. Fischer and U. Heinbuch, Relationship between free energy density functional, Born-Green-Yvon, and potential distribution approaches for inhomogeneous fluids, *J. Chem. Phys.*, **88** (1988), 1909–1913.
[25] D. Gillespie and R. S. Eisenberg, Physical descriptions of experimental selectivity measurements in ion channels, *European Biophys. J.*, **31** (2002), 454–466.
[26] D. Gillespie, *A Singular Perturbation Analysis of the Poisson-Nernst-Planck System: Applications to Ionic Channels,* Ph. D Dissertation, Rush University at Chicago, 1999.
[27] D. Gillespie, W. Nonner and R. S. Eisenberg, Coupling Poisson-Nernst-Planck and density functional theory to calculate ion flux, *J. Phys.: Condens. Matter*, **14** (2002), 12129–12145.
[28] D. Gillespie, W. Nonner and R. S. Eisenberg, Density functional theory of charged, hard-sphere fluids, *Phys. Rev. E*, **68** (2003), 0313503 (1-10).
[29] D. Gillespie, W. Nonner and R. S. Eisenberg, Crowded charge in biological ion channels, *Nanotech,* **3** (2003), 435–438.
[30] E. Gongadze, U. van Rienen, V. Kralj-lglič and A. lglič, Spatial variation of permittivity of an electrolyte solution in contact with a charged metal surface: A mini review, *Computer Method in Biomechanics and Biomedical Engineering*, **16** (2013), 463–480.
[31] D. Gillespie, L. Xu, Y. Wang and G. Meissner, (De)constructing the Ryanodine Receptor: Modeling Ion Permeation and Selectivity of the Calcium Release Channel, *J. Phys. Chem. B*, **109** (2005), 15598–15610.
[32] U. Hollerbach, D.-P. Chen and R. S. Eisenberg, Two- and three-dimensional Poisson-Nernst-Planck simulations of current flow through gramicidin-A, *J. Comp. Science*, **16** (2002), 373–409.
[33] U. Hollerbach, D. Chen, W. Nonner and B. Eisenberg, Three-dimensional Poisson-Nernst-Planck Theory of Open Channels, *Biophys. J.,* **76** (1999), p. A205.
[34] Y. Hyon, B. Eisenberg and C. Liu, A mathematical model for the hard sphere repulsion in ionic solutions, *Commun. Math. Sci.*, **9** (2011), 459–475.
[35] Y. Hyon, J. Fonseca, B. Eisenberg and C. Liu, Energy variational approach to study charge inversion (layering) near charged walls, *Discrete Contin. Dyn. Syst. Ser. B,* **17** (2012), 2725–2743.
[36] Y. Hyon, C. Liu and B. Eisenberg, PNP equations with steric effects: A model of ion flow through channels, *J. Phys. Chem. B,* **116** (2012), 11422–11441.
[37] W. Im, D. Beglov and B. Roux, Continuum solvation model: Electrostatic forces from numerical solutions to the Poisson-Bolztmann equation, *Comp. Phys. Comm.*, **111** (1998), 59–75.

[38] W. Im and B. Roux, Ion permeation and selectivity of OmpF porin: A theoretical study based on molecular dynamics, Brownian dynamics, and continuum electrodiffusion theory, *J. Mol. Biol.*, **322** (2002), 851–869.
[39] S. Ji and W. Liu, Poisson-Nernst-Planck systems for ion flow with density functional theory for hard-sphere potential: I-V relations and critical potentials. Part I: Analysis, *J. Dyn. Diff. Equat.*, **24** (2012), 955–983.
[40] S. Ji, W. Liu and M. Zhang, Effects of (small) permanent charges and channel geometry on ionic flows via classical Poisson-Nernst-Planck models, *SIAM J. on Appl. Math.,* **75** (2015), 114–135.
[41] Y. Jia, W. Liu and M. Zhang, Qualitative properties of ionic flows via Poisson-Nernst-Planck systems with Bikerman's local hard-sphere potential: Ion size effects, *Discrete and Continuous Dynamical Systems-B,* **21** (2016), 1775–1802.
[42] M. S. Kilic, M. Z. Bazant and A. Ajdari, Steric effects in the dynamics of electrolytes at large applied voltages. II. Modified Poisson-Nernst-Planck equations, *Phys. Rev. E*, **75** (2007), 021503 (11 pages).
[43] A. S. Khair and T. M. Squires, Ion steric effects on electrophoresis of a colloidal particle, *J. Fluid Mech.,* **640** (2009), 343–356.
[44] C.-C. Lee, H. Lee, Y. Hyon, T.-C. Lin and C. Liu, New Poisson-Boltzmann type equations: One-dimensional solutions, *Nonlinearity*, **24** (2011), 431–458.
[45] B. Li, Continuum electrostatics for ionic solutions with non-uniform ionic sizes, *Nonlinearity*, **22** (2009), 811–833.
[46] W. Liu, Geometric singular perturbation approach to steady-state Poisson-Nernst-Planck systems, *SIAM J. Appl. Math.,* **65** (2005), 754–766.
[47] W. Liu, One-dimensional steady-state Poisson-Nernst-Planck systems for ion channels with multiple ion species, *J. Differential Equations*, **246** (2009), 428–451.
[48] G. Lin, W. Liu, Y. Yi and M. Zhang: Poisson-Nernst-Planck systems for ion flow with density functional theory for local hard-sphere potential, *SIAM J. Appl. Dyn. Syst.*, **12** (2013), 1613–1648.
[49] W. Liu, X. Tu and M. Zhang, Poisson-Nernst-Planck Systems for Ion Flow with Density Functional Theory for Hard-Sphere Potential: I-V relations and Critical Potentials. Part II: Numerics, *J. Dyn. Diff. Equat.*, **24** (2012), 985–1004.
[50] W. Liu and B. Wang, Poisson-Nernst-Planck systems for narrow tubular-like membrane channels, *J. Dyn. Diff. Equat.,* **22** (2010), 413–437.
[51] W. Liu and H. Xu, A complete analysis of a classical Poisson-Nernst-Planck model for ionic flow, *J. Differential Equations,* **258** (2015), 1192–1228.
[52] W. Nonner and R. S. Eisenberg, Ion permeation and glutamate residues linked by Poisson-Nernst-Planck theory in L-type Calcium channels, *Biophys. J.*, **75** (1998), 1287–1305.
[53] S. Y. Noskov, W. Im and B. Roux, Ion Permeation through the $z_1$-Hemolysin Channel: Theoretical Studies Based on Brownian Dynamics and Poisson-Nernst-Planck Electrodiffusion Theory, *Biophys. J.*, **87** (2004), 2299–2309.
[54] S. Y. Noskov and B. Roux, Ion selectivity in potassium channels, *Biophys. Chem.,* **124** (2006), 279–291.
[55] B. Nadler, Z. Schuss, A. Singer and B. Eisenberg, Diffusion through protein channels: From molecular description to continuum equations, *Nanotech.,* **3** (2003), 439–442.
[56] J. K. Percus, Equilibrium state of a classical fluid of hard rods in an external field, *J. Stat. Phys.*, **15** (1976), 505–511.
[57] J. K. Percus, Model grand potential for a nonuniform classical fluid, *J. Chem. Phys.*, **75** (1981), 1316–1319.
[58] J.-K. Park and J. W. Jerome, Qualitative properties of steady-state Poisson-Nernst-Planck systems: Mathematical study, *SIAM J. Appl. Math.*, **57** (1997), 609–630.
[59] B. Roux, T. W. Allen, S. Berneche and W. Im, Theoretical and computational models of biological ion channels, *Quat. Rev. Biophys.*, **37** (2004), 15–103.
[60] Y. Rosenfeld, Free-energy model for the inhomogeneous hard-sphere fluid mixture and density-functional theory of freezing, *Phys. Rev. Lett.*, **63** (1989), 980–983.
[61] Y. Rosenfeld, Free energy model for the inhomogeneous fluid mixtures: Yukawa-charged hard spheres, general interactions, and plasmas, *J. Chem. Phys.*, **98** (1993), 8126–8148.
[62] R. Roth, Fundamental measure theory for hard-sphere mixtures: A review, *J. Phys.: Condens. Matter*, **22** (2010), 063102 (1–18).

[63] A. Singer, D. Gillespie, J. Norbury and R. S. Eisenberg, Singular perturbation analysis of the steady-state Poisson-Nernst-Planck system: applications to ion channels, *European J. Appl. Math.,* **19** (2008), 541–560.
[64] A. Singer and J. Norbury, A Poisson-Nernst-Planck model for biological ion channels–an asymptotic analysis in a three-dimensional narrow funnel, *SIAM J. Appl. Math.*, **70** (2009), 949–968.
[65] Z. Schuss, B. Nadler and R. S. Eisenberg, Derivation of Poisson and Nernst-Planck equations in a bath and channel from a molecular model, *Phys. Rev. E*, **64** (2001), 036116.
[66] X.-S. Wang, D. He, J. Wylie and H. Huang, Singular perturbation solutions of steady-state Poisson-Nernst-Planck systems, *Phys. Rev. E,* **89** (2014), 022722 (1–14).
[67] G. W. Wei, Q. Zheng, Z. Chen and K. Xia, Variational multiscale models for charge transport, *SIAM Review*, **54** (2012), 699–754.
[68] J. Zhang, D. Acheampong and M. Zhang, Geometric singular approach to Poisson-Nernst-Planck models with excess chemical potentials: Ion size effects on individual fluxes, *Mol. Based Math. Biol.*, **5** (2017), 58–77.
[69] M. Zhang, Asymptotic expansions and numerical simulations of I-V relations via a steady-state Poisson-Nernst-Planck system, *Rocky Mountain J. Math.,* **45** (2015), 1681–1708.
[70] Q. Zheng and W. Wei, Poisson-Boltzmann-Nernst-Planck model, *J. Chem. Phys.*, **134** (2011), 194101 (1–17).

Received May 2017; 1st revision August 2017, 2nd revision September 2017.

*E-mail address*: ljwenling@163.com
*E-mail address*: liji@hust.edu.cn
*E-mail address*: Joseph.Shackelford@student.nmt.edu
*E-mail address*: Jeremy.Vorenberg@student.nmt.edu
*E-mail address*: mingji.zhang@nmt.edu, mzhang0129@gmail.com

# Recommendation letters for Jeremy Vorenberg for Langmuir Award

Dear committee members,

It is my pleasure to write this recommendation letter in support of Jeremy Vorenberg, a double major undergraduate student (Electrical Engineering and Mathematics) for the Langmuir Award.

I got to know Jeremy since August, 2015 when he took my Calculus III class. He also took Math 335 Ordinary Differential Equations and Math 352, Basic Concepts of Mathematics, Math 336 Introduction to Partial Differential Equations, Math 430 Mathematical Modeling, Math 437, Systems of Ordinary Differential Equations and Math 531 Special Topics in Ordinary Differential Equations with me. I was surprised by his hard work on the courses, the ability in analyzing and solving complicated problems, and his excellent performances (All A's for the courses, actually, $A^+$). Jeremy also demonstrated good teamwork skills in group assignments. His current GPA is **3.97/4.0**, which is excellent.

In particular, when he took my Math 531 in Spring 2017, he started to work on a research project related to the qualitative properties of ionic flows through ion channels via Poisson-Nernst-Planck systems without assuming the so-called electroneutrality conditions. We completed the project and submitted to a top professional mathematical journal **Discrete and Continuous Dynamical Systems Series B,** and now the paper is published online first and will appear sometime this August. The information of the paper can be found using the following link

http://aimsciences.org/article/doi/10.3934/dcdsb.2018064

I will attach the paper together with this letter for your convenience. His contribution in this work is more than 40%, and I believe for a third-year undergraduate student, this is just wonderful. He has been doing even a better job compared to our many graduate students. As his advisor in mathematics, I am so proud of him!

I personally believe Jeremy Vorenberg is an excellent candidate for the award. I would like to strongly recommend Jeremy Vorenberg for Langmuir Award.

For any further concerns about this letter, please do not hesitate to contact me.

Mingji Zhang

Assistant Professor of Mathematics

New Mexico Tech

Email: Mingji.zhang@nmt.edu